Computational Characterization and Model Verification for 3D Microstructure Reconstruction of Additively-Manufactured Materials

Arulmurugan Senthilnathan*
Virginia Tech, Blacksburg, 24061, VA, USA

Iman Javaheri†, Veera Sundararaghavan‡
University of Michigan, Ann Arbor, 48109, MI, USA

Pınar Acar§
Virginia Tech, Blacksburg, 24061, VA, USA

The goal of this study is to characterize and validate the texture and grain topology of additively-manufactured anisotropic three-dimensional (3D) polycrystalline microstructures. The special focus is on developing methodologies to compare the grain shapes and orientations of two-dimensional (2D) and 3D microstructure representations using the same metric. To generate statistical data, synthetic microstructures are reconstructed from experimental data using Markov random field (MRF). The statistical similarity between the experimental and synthetic microstructures is verified by comparing their grain topologies. A universal measure to compare 2D and 3D grains is portrayed through the concept of image moments that are invariant to shape transformations. The graphical plots developed based on moment invariants to compare the 2D and 3D grains are used to verify the synthetic model.

Nomenclature

μ	=	Central moment
η	=	Normalized central moment
η_x	=	Normalized central moment in x direction for 3D grains
η_y	=	Normalized central moment in y direction for 3D grains
η_z	=	Normalized central moment in z direction for 3D grains

I. Introduction

Additively-manufactured materials demonstrate complex microstructural features, such as texturing and grain topology [1–3]. Since additive manufacturing procedures are expensive and time-consuming, computational reconstruction of microstructures [4–18] saves significant cost and time to generate materials data in large domains. These computational reconstruction techniques produce statistically equivalent microstructures with respect to the microstructural features of experimental images. The goal in the present work focuses on characterizing and comparing the grain topologies of two-dimensional (2D) experimental images and three-dimensional (3D) reconstructed anisotropic microstructures using image moments. To achieve this goal, the computational reconstruction of two anisotropic microstructures manufactured by different techniques are considered. One is additively-manufactured 316L stainless steel and another is a rolled aluminum-lithium (Al-Li) alloy sample.

Conventionally, electron backscatter diffraction (EBSD) [20–25] method produces a clear view of the microstructural features of metallic materials, including the orientation information represented in the red-green-blue (RGB) color

*Graduate Research Assistant, Ph.D. Student, Department of Mechanical Engineering. AIAA Student Member

†Ph.D. Student, Department of Aerospace Engineering; also Student Trainee, Durability, Damage Tolerance, and Reliability Branch, NASA Langley Research Center, Hampton, VA 23681. AIAA Student Member

‡Professor, Department of Aerospace Engineering. AIAA Member

§Assistant Professor, Department of Mechanical Engineering. AIAA Member

channels through the inverse pole figure (IPF) method. Nevertheless, laborious sample preparation procedures that result in material waste are necessary to operate the instruments required to generate the EBSD data. Furthermore, EBSD scanning techniques necessitate a near-perfect clean surface in order to extract orientation information via IPF coloring, which is required for reconstruction methods.

Computational microstructure reconstruction algorithms minimize the cost and time requirements of large-scale experiments. They predict microstructural evolution in large spatial domains using small-scale experimental information. Generation of synthetic microstructures has been achieved in the past through many methods including statistical correlation functions [4, 5], physical descriptors [6, 7], and Gaussian methods [8, 9]. Moreover, advanced machine learning methods [10–12] have also been explored for the prediction of microstructural evolution. The Markov random field (MRF) is found to be an efficient approach that requires fewer experimental data samples. The MRF method has been implemented before for the prediction of the large-scale spatial and spatio-temporal evolution of 2D [13, 14] and 3D [15–17] microstructure maps for polycrystalline materials. Interested readers are referred to [26] for an elaborated review of the state-of-the-art techniques for microstructure characterization and reconstruction (MCR) methods.

The randomness in the MRF algorithm introduces stochasticity into the reconstructed microstructure. In particular, each reconstructed microstructure sample by the MRF algorithm using the same experimental data may appear slightly different. This introduces variations to the microstructural features and resulting homogenized properties. Hence, it is crucial to investigate the reconstructed microstructure that is expected to be statistically equivalent to the experimental data. While our previous studies [27, 28] focused on the reconstruction of isotropic microstructures, the current work explores the challenges in verifying the reconstruction of rolled and additively-manufactured anisotropic microstructures with respect to the 2D orthogonal experimental images.

The macroscopic properties and performance of materials are driven by the underlying micro-level features such as the texture and grain topology. The grain size and shape of a polycrystalline microstructure have a significant impact on homogenized material behavior. While the Hall-Petch effect [19] has been used to account for grain size, the effects of grain shapes, particularly in complex microstructures including additively-manufactured materials, are still under investigation. Multiple descriptors have been developed in the past to represent grain shapes. Some of these include two-point statistical correlation functions [4], Fourier analysis [29], Minkowski functions [30, 31], and some experimental techniques [32]. However, the aforementioned methods do not capture the grain shape explicitly. The concept of image moment exceeds the performance of all other descriptors due to its invariant property. For different shape transformations, certain types of image moments are invariant to rotation, translation, and scale (RST) of shapes. Hence, the use of moment invariants as shape descriptors has huge advantages and therefore has been explored before [33–41] where these image moments were applied to compare grain shapes (both 2D and 3D) to common geometric shapes, such as ellipses, circles, and rectangles, by introducing a second order moment invariant map (SOMIM) [34–36], and to precipitate shapes [40, 41]. The present work introduces the preliminary work of the authors [42] by utilizing normalized central moments (η) to compare the grain topology of 2D and 3D microstructure representations.

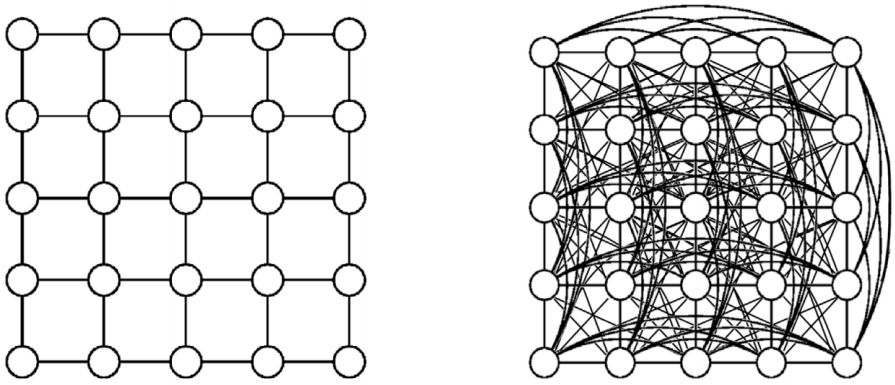
The paper is structured as follows. The methodology to reconstruct synthetic 3D anisotropic microstructures is described in Section II, followed by the formulation for quantification of grain shapes through moment invariants. Next, the MRF reconstructed results and the validation procedure are outlined in Section III. The observations are discussed in more detail in Section IV. Thereafter, a summary of this work as well as future plans contained in Section V.

II. Methodology

A. Microstructure Reconstruction with Markov Random Field

MRF is an undirected graphical model. 2D images are constructed as a graphical model where the pixels are represented as nodes that are connected to each other. An image of $n \times n$ dimensions is described as an Ising model [43] of the same size. The lattice points of the model represent the pixel intensity values with values X_i containing any one of G color levels in the range of $0, 1, ..., G-1$ of the image and the nodes are connected through a conditional dependence. Fig. 1a represents a simple connection between the nodes. However, for reconstruction through MRF, higher-order interactions, as illustrated in Fig. 1b, are introduced between the lattice points. The local Markovian property, which states that the probability of a value (X) is conditionally independent of all other values outside of its neighbors, represents the joint probability density of all points.

This work follows the 3D reconstruction technique presented in Ref. [16, 17]. The conditional probability density determines the color of an unknown voxel by calculating the most probable RGB pixel value. The pixel intensity value is predicted by locating a window of a user-defined size in the input 2D image that is similar to the unknown neighborhood



(a) (b)

Fig. 1 MRF as an undirected graphical model. The circles show the pixels of an image. The bonds are used to connect the neighbors: (a) Ising model with the nearest-neighbor interactions, (b) a higher-order Ising model. The microstructure reconstruction performed in this work is based on the MRF method, which is a higher-order Ising model.

of each voxel in all three directions. Similar information is acquired for other directions from respective 2D sections for an anisotropic microstructure. Within the experimental images, there are three best-matching neighbors for each voxel. The best color is found by setting the derivative of the energy function [16, 17] to zero with regard to a weighted average expression to find the unique value of the unknown voxel. A set of three 2D orthogonal images are used to reconstruct the 3D microstructures (Fig. 2). This work utilizes experimental images of two different materials to demonstrate the reconstruction and validation procedures. One is a rolled sample made of an Al-Li alloy (Fig. 2(a)) and another is an additively-manufactured sample of 316L stainless steel (Fig. 2(b)). More information about the aforementioned materials utilized in this work can be found in previous works [16, 17].

The resulting 3D anisotropic microstructures reconstructed from the experimental 2D orthogonal images are presented in Fig. 2 for both materials. For convenience, the directions of the rolled sample are discussed using longitudinal (L), short transverse (ST), and long transverse (LT) notations and the directions of the additively-manufactured sample are denoted with conventional X (scanning direction), Y (building direction), and Z (transverse direction) signs. The 2D images of both materials exhibit different textures in all three planes normal to the three directions. While the surfaces of the generated 3D microstructure do give visual resemblance to the textures of the three orthogonal images, it is necessary to statistically compare the synthetic texture of 2D and 3D microstructures. To compare the grain shapes, the microstructures are initially divided into ten distinct clusters, each of which has a collection of grains with the same orientation. The noise observed in 3D grain clusters (Fig. 3) is removed by defining a threshold value for the number of pixels before characterizing the features with moment invariants. Each grain is then isolated from the clusters for individual shape quantification. An example of clusters for the 3D reconstructed additively-manufactured microstructure is presented in Fig. 3. Nevertheless, a metric is required to compare the grain shapes of the original 2D sample and 3D anisotropic reconstruction. This challenge can be addressed by quantifying the grain shapes using the concept of moment invariants.

B. Quantification of Grain Shapes

The physical concept of the moment for an image describes the distribution of pixel intensities of an image. Certain types of moments possess an invariant property to the different transformations of grain shapes. The invariant parameters can capture the shapes of physical objects with a numerical representation. One such type is known as the central moment (μ), which statistically resembles variance and is formulated in Eq. (1). μ is invariant to the translation of shapes. By normalizing μ over the image area (A), which is defined as the summation of all pixel intensities, a normalized central moment (η) is derived (Eq. (2)). In addition to translation, η is also scale-invariant for shapes. Irrespective of dimensions, η is measured in one particular direction capturing the normalized variance of the grain in that direction. Both 2D and 3D grains can be quantified using the same measure, η, which is also an invariant parameter

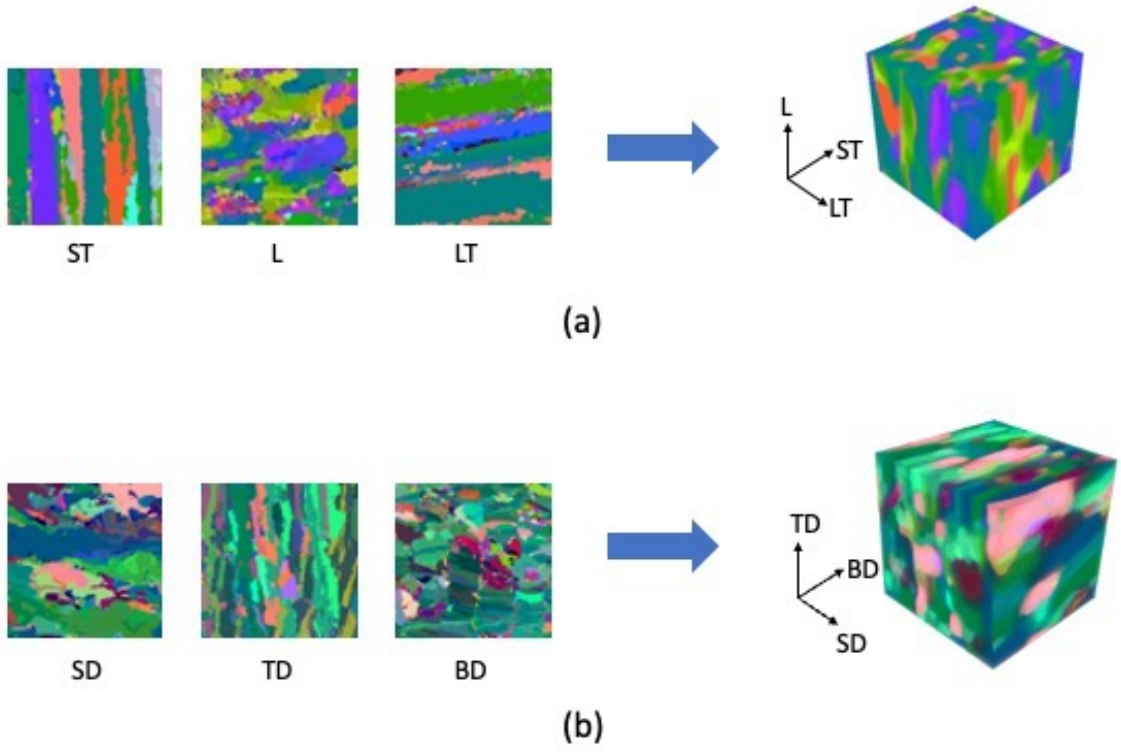


Fig. 2 Reconstruction of 3D microstructures from three orthogonal 2D images: (a) Rolled Al-Li sample (b) Additively-manufactured 316L stainless steel sample.

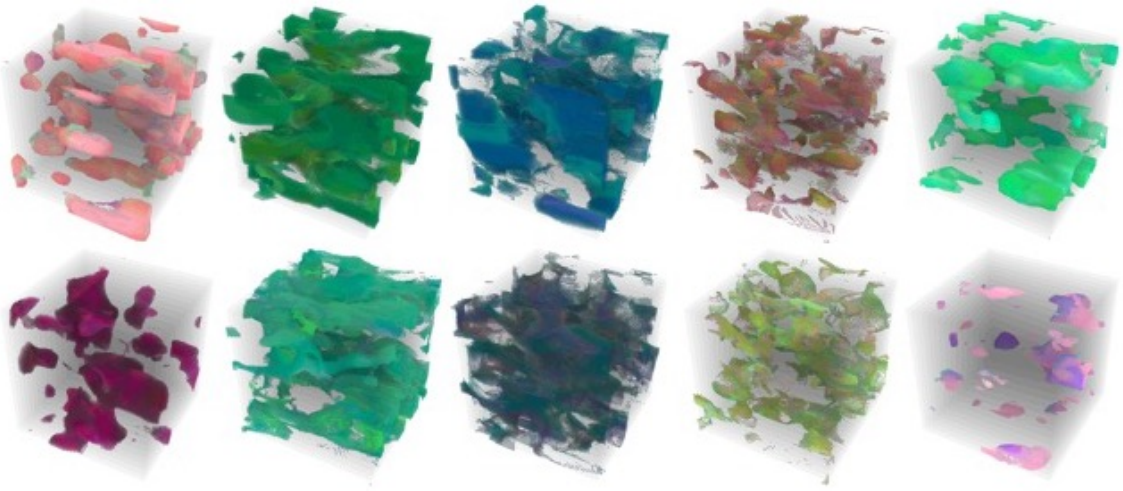


Fig. 3 Clusters of the reconstructed 3D microstructure from three orthogonal 2D images of additively-manufactured 316L stainless steel sample presented in Ref. 2.

to different transformations. Equations (1) and (2) are formulated to calculate μ and η, respectively for 3D grains. For 2D grains, the z-direction-related components of Eq. (1) and Eq. (2) are eliminated.

$$\mu_{ijk} = \sum_{x}\sum_{y}\sum_{z}(x-\bar{x})^{i}(y-\bar{y})^{j}(z-\bar{z})^{k}I(x,y,z) \tag{1}$$

$$\eta_{ijk} = \frac{\mu_{ijk}}{(Volume)^{\gamma}} \text{ where } \gamma = \frac{2+i+j+k}{2} \tag{2}$$

III. Results

The MRF algorithm is programmed to generate synthetic microstructures that are statistically equivalent to the input (in this study, experimental) images. Hence, it is important to compare the statistics of the reconstructed and experimental microstructures. The validation of the reconstructed microstructure is performed by comparing 2D and 3D grain shapes. The presented method builds upon a previous methodology we established for isotropic microstructures [42]. While the previous work compares the 2D and 3D isotropic microstructures using principle eigenvalue moments to validate the synthetic samples, the present work proposes to use normalized central moments (η), which can be a universal measure to quantify grain shapes along different dimensions. Using the same metric (η), the distributions of the 2D and 3D grains are compared first. Then, a demonstration of the box whisker plot is used to compare the shapes and orientations of the 2D and 3D grains in detail.

First, each of the 2D and 3D grains separated from their clusters is quantified through η in all three directions. Since MRF is developed using a Gaussian-distributed weight parameter [13], the synthetic microstructure is also expected to produce a texture with a similar distribution. Evidently, the grains of both materials quantified using the lognormal transformation of η exhibit a normal distribution as presented in Figs. 4 and 5. The logarithmic value of η is negative because naturally, the η values are less than 1 due to a large image area. Each of the three distribution curves of the 3D microstructure (Fig. 4(b) and Fig. 5(b)) is compared to its counterpart in 2D distributions. For example, η_x of the 3D microstructure representing the normalized variations of all the 3D grains in the x-direction is compared to the η_x of 2D grains obtained for the xy and xz planes i.e, the planes normal to the direction of LT (xz-plane) and L (xy-plane). The distributions of 2D η_x for both xz and xy planes and the distribution of 3D η_x are found to be comparable (Figs. 4 and 5). A similar comparison can be made for the η_y and η_z distributions (Figs. 4 and 5).

Next, the shape and orientation of 2D and 3D grains are compared using the same metric (η_x, η_y, and η_z). A box whisker plot is constructed using the $|\ln \eta|$ values and presented in Fig. 6 and Fig. 7 for the rolled and additively-manufactured microstructure samples, respectively. The normalized variances of both 2D and 3D grains quantified by the invariant η are compared in all three directions. For 2D grains, the normalized variance in a direction is spread out in two planes. That is, the net η_x value of 2D grain is resolved into the planes normal to LT (xz-plane) and L (xy-plane) directions. Therefore, three box whisker plots are created for each sample to individually compare the data. For example, as illustrated in Fig. 6 and Fig. 7, the planes normal to the ST direction (yz-plane) contain the information about the spread and skewness of all the 2D and 3D grains in both y and z directions. The η is the same measure quantifying both shape and orientation (represented by pixel intensities) of 2D and 3D grains making it advantageous over other moments. The box whisker plot provides an analysis of the grain shape comparison for each plane individually, which makes it preferable for the case of anisotropic microstructures.

IV. Discussion

The parameter η is suitable for quantifying grains because it is invariant to both shape and orientation. Additionally, η can serve as a universal parameter to measure the grain shapes of different dimensions. The natural logarithmic values of η quantifying the grains are found to have a normal distribution that is commensurate to the way the MRF algorithm is constructed. Hence, lognormal distributions of the grains are compared in Fig. 4 and Fig. 5 for rolled and additively-manufactured samples, respectively. The distribution curves are color-coded to compare the directions. The distribution lines of 2D orthogonal images have different shades to denote the three planes. Each of the distribution curves in Figs. 4 and 5 for both 2D and 3D grains demonstrates the normal distribution. For both samples (rolled and additively-manufactured), as presented in Figs. 4 and 5, the distribution of synthetic 3D grains are matching with its corresponding counterpart directions in the 2D images. Therefore, all the grains in the 2D and 3D microstructures are varying proportionally in the three directions. Next, more information about the spread of the grains is found in the box whisker plot.

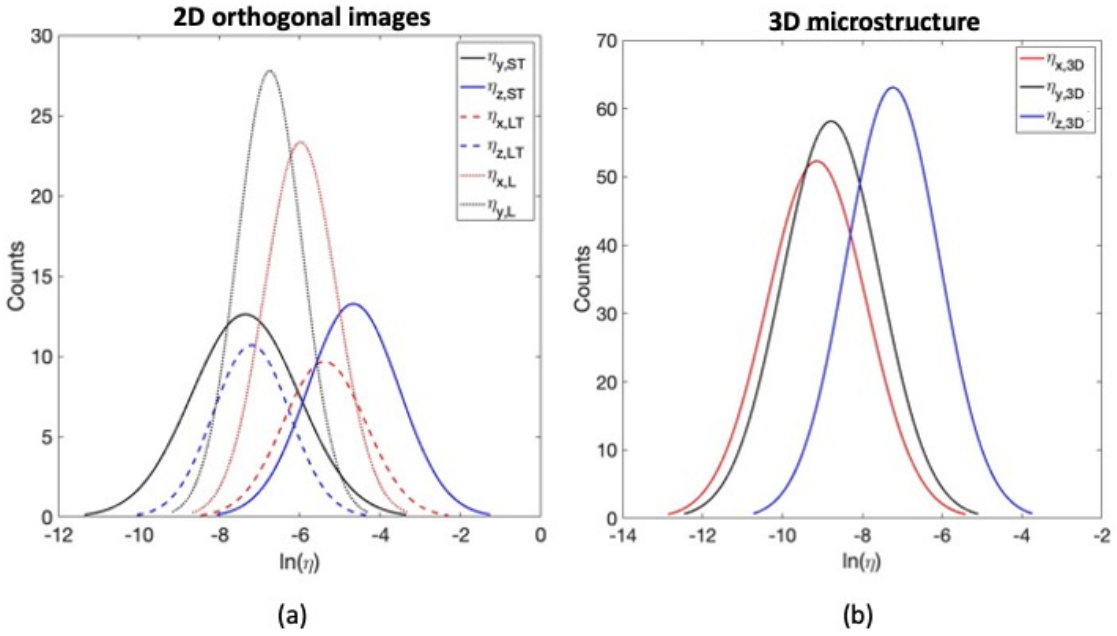


Fig. 4 Distributions of 2D and 3D microstructures of rolled sample.

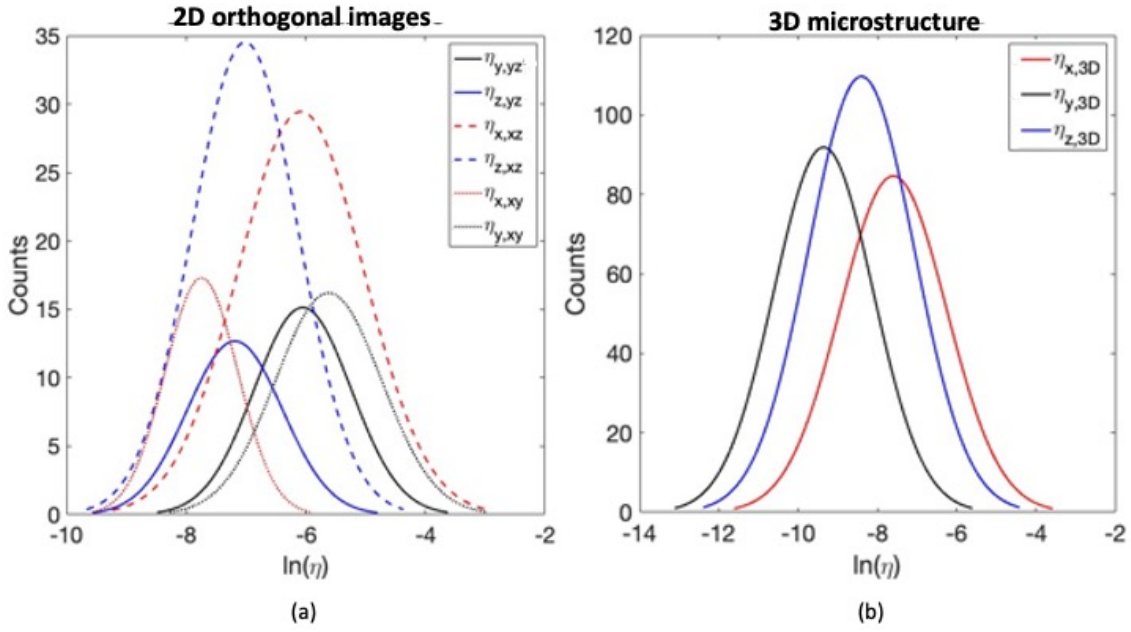


Fig. 5 Distributions of 2D and 3D microstructures of additively-manufactured sample.

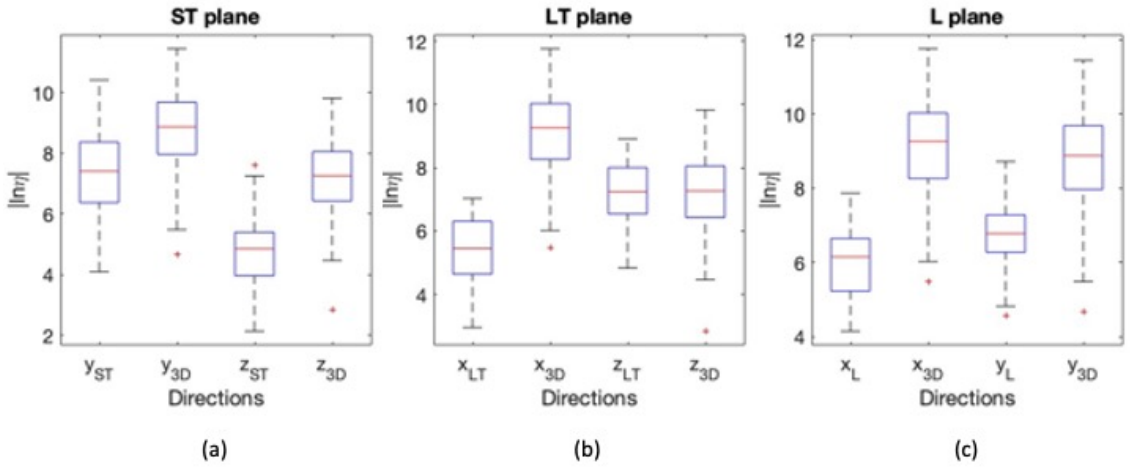


Fig. 6 Box and whisker plot of 2D and 3D microstructures of rolled samples.

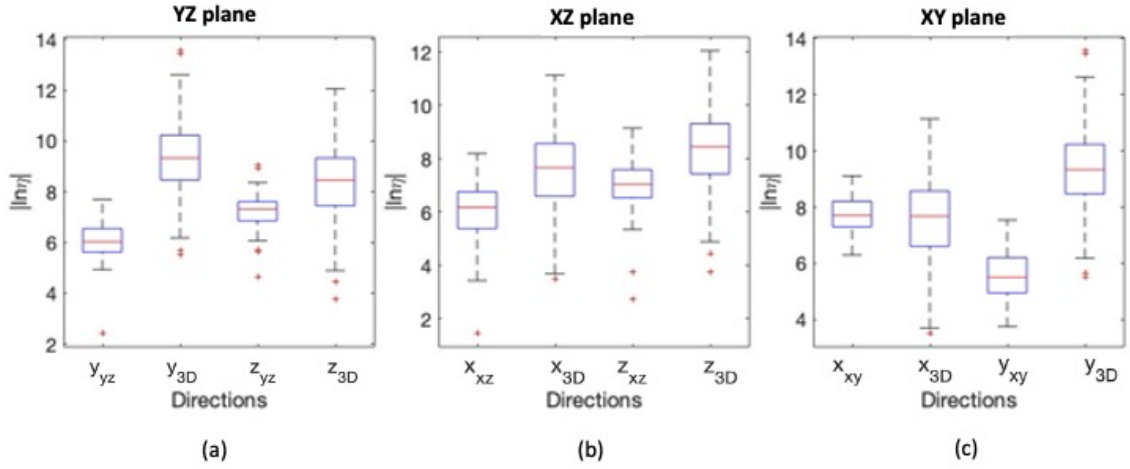


Fig. 7 Box and whisker plot of 2D and 3D microstructures of additively-manufactured sample.

First, for the rolled sample, the spread of normalized variance in the z direction of 2D grains in the LT plane (z_{LT}) is found to be completely within the range of the normalized variance of 3D grains in the z direction (z_{3D}). Both $\eta_{z,LT}$ and $\eta_{z,3D}$ have no skewness, thus agreeing with a normal distribution. The long transverse direction (y) also has the 2D and 3D grains varying commensurate to each other. This can be found in the plots of $\eta_{y,ST}$ vs $\eta_{y,3D}$ in the ST plane (Fig. 6) and $\eta_{y,L}$ vs $\eta_{y,3D}$ in the L plane (Fig. 7). The slight mismatch between the η_y values of 2D and 3D grains in both the ST and L plane for the aforementioned comparison can be attributed to the large volume of the 3D grains. However, when it comes to the normalized variance of 2D and 3D grains in the x direction, the spread of 3D grains is translated slightly away from the range of 2D grains both in the LT and L planes. The 2D grains varying in the x direction of the LT and L planes and the z direction of the ST plane are found to be slightly skewed to the left. Their counterpart directions in the 3D microstructure (η_z and η_x), although not visible in Fig. 6, do produce a slightly left-skewed distribution.

Next, for the additively-manufactured sample, the small boxes for 2D cases in box whisker plots of Fig. 7 imply that the shapes of 2D grains are similar to each other. When compared with 3D, the 2D grains are varying proportionately to the 3D grains in both x and z directions. The spread and skewness of η_x in xz and xy planes, and η_z in yz and xz planes for both 2D and 3D grains are found to be analogous. On the other hand, the Y direction has a slight anomaly indicating that the reconstruction has provided more similar microstructural features to the experimental data in x and z directions. The outliers present in Fig. 6 and Fig. 7 simply represent the corner grains and grains with unusual shapes compared to the other 2D and 3D grains. An example of an outlier grain is presented in Fig. 8.



Fig. 8 An outlier grain from the experimental z_{xz} data of Fig. 7. Here, the orientations of all pixels are very similar. As a result, the clustering algorithm considered them to be the same grain.

The synthetic microstructures generated by the MRF algorithm demonstrate features that are statistically equivalent to the input (experimental) microstructure. Therefore, it becomes crucial to analyze how much the shape and orientation of synthetic 3D grains are varying with respect to the 2D grains. The statistical parameters from the distribution data (Fig. 4 and Fig. 5) of both materials are determined and listed in Table 1 to understand the anisotropic nature of the reconstructed microstructure. The parameters describing 3D grains are compared to 2D grains for each direction. The notation for the 2D grain directions in Table 1 is as follows: $\text{direction}_{\text{plane}}$. The mean value can be used to find how much the 3D grains are offset from the 2D grains. The standard deviation and variance measure how much the 3D grains are varying from the distributions of the 2D grains in a particular direction. For example, it is worth noting that for the rolled sample, the mean of 3D grains offsetted more from the mean of 2D grains in the X direction compared to the other two. For the additively-manufactured sample, the mean of 3D grains has offsetted more in the Y direction than the other two which is analogous to the observation made from the box whisker plot of the additively-manufactured sample. Furthermore, in the case of the rolled sample, it is observed that the variance of 3D grains in the Z direction (L) is close to the variance of the 2D grains in the Z direction of the yz plane (ST) than the Z direction of the xz plane (LT). From this observation, it can be concluded that the reconstruction works better on the yz plane rather than the xz plane for the rolled sample. The mean and variance values demonstrate that the algorithm produces 3D features that are more statistically equivalent to the experimental orthogonal images in some directions than others. These statistics are better characterized with larger databases of reconstructed samples in the future. The generation of statistical data will also enable to study the propagation of the algorithmic uncertainty of the MRF method on synthetic anisotropic microstructures.

Table 1 Statistical parameters of 2D and 3D grains quantified by η in all the three directions.

Method	Parameter	X			Y			Z		
		3D	X_{xz}	X_{xy}	3D	Y_{yz}	Y_{xy}	3D	Z_{yz}	Z_{xz}
Rolled	Mean	9.13848	5.380784	5.976988	8.779185	7.350776	6.743291	7.231071	4.660436	7.197765
	Standard deviation	1.242754	1.028651	0.89541	1.228236	1.334567	0.808697	1.164793	1.13509	0.951241
	Variance	1.544438	1.058122	0.80176	1.508564	1.78107	0.65399	1.356743	1.288429	0.90486
Additively manufactured	Mean	7.595243	6.080227	7.747056	9.357121	6.049683	5.61661	8.402375	7.185405	7.015467
	Standard deviation	1.339053	1.051975	0.608671	1.251892	0.811646	0.888308	1.330783	0.795874	0.884797
	Variance	1.793062	1.106652	0.370481	1.567235	0.658770	0.789092	1.770984	0.633415	0.782866

V. Summary

The present work addresses the validation of the 3D anisotropic microstructures by statistically comparing them to the experimental 2D orthogonal images. The special focus is on the 3D reconstruction of Al-Li and 316L stainless steel alloys. The 3D synthetic microstructures are generated using the Markov random field algorithm. To compare the 2D and 3D grains, a universal metric that are invariant to shape transformations is used. The synthetic microstructures are compared to the experimental images in three planes normal to the X, Y, and Z directions. The distributions of 2D and 3D grain shapes quantified by η are found to be similar. The grain topologies are compared in each direction through a box whisker plot. Statistical measures derived from the distributions of grain shapes quantified by η are used to understand the anisotropic features of the reconstructed microstructures. For future work, more synthetic samples can be generated to investigate the effects of the algorithmic uncertainty of MRF on microstructural features in large computational domains.

VI. Acknowledgments

The authors thank Prof. John Allison from the Materials Science and Engineering Department of the University of Michigan for providing experimental microstructure images. Arulmurugan Senthilnathan and Pınar Acar would like to acknowledge the financial support from the Air Force Office of Scientific Research (AFOSR) Young Investigator Program under Grant FA9550-21-1-0120. Iman Javaheri and Veera Sundararaghavab also wish to acknowledge the financial support from the AFOSR, Materials for Extreme Environments Program under Grant FA9550-22-1-0319.

References

[1] Wong, K.V., and Hernandez, A., "A review of additive manufacturing", *International scholarly research notices*, 2012.

[2] Frazier, W. E., "Metal additive manufacturing: a review", *Journal of Materials Engineering and performance*, Vol. 23, No. 6, 2014, pp. 1917-1928.

[3] Gibson, I., Rosen, D. W., Stucker, B., Khorasani, M., Rosen, D., Stucker, B., and Khorasani, M., "Additive manufacturing technologies", Vol. 17, *Springer*, Cham, Switzerland, 2021.

[4] Choudhury, A., Yabansu, Y.C., Kalidindi, S.R. and Dennstedt, A., "Quantification and classification of microstructures in ternary eutectic alloys using 2-point spatial correlations and principal component analyses", *Acta Materialia*, Vol. 110, May 2016, pp: 131-141.

[5] Liu, Y., Greene, M.S., Chen, W., Dikin, D.A. and Liu, W.K., "Computational microstructure characterization and reconstruction for stochastic multiscale material design", *Computer-Aided Design*, Vol. 45, No. 1, 2013, pp: 65-76.

[6] Xu, H., Li, Y., Brinson, C. and Chen, W., "Descriptor-based methodology for designing heterogeneous microstructural materials system", *American Society of Mechanical Engineers Digital Collection*, 2013.

[7] Xu, H., Dikin, D.A., Burkhart, C. and Chen, W., "Descriptor-based methodology for statistical characterization and 3D reconstruction of microstructural materials", *Computational Materials Science*, Vol. 85, April 2014, pp: 206-216.

[8] Zhen, J., Chen, W., and Burkhart, C., "A hybrid approach to 3D porous microstructure reconstruction via Gaussian random field", *American Society of Mechanical Engineers Digital Collection*, 2012.

[9] Jiang, Z., Chen W., and Burkhart, C., "Efficient 3D porous microstructure reconstruction via Gaussian random field and hybrid optimization", *Journal of microscopy*, Vol. 252, No. 2, 2013, pp: 135-148.

[10] Ashton, T. N., Guillen, D. P., and Harris, W. H., "An algorithm to generate synthetic 3D microstructures from 2D exemplars", *JOM*, Vol. 72, No. 1, 2020, pp: 65-74.

[11] Xiaolin, L., Zhang, Y., Zhao, H., Burkhart, C., Brinson, L. C., and Chen, W., "A transfer learning approach for microstructure reconstruction and structure-property predictions", *Scientific reports 8*, no. 1, 2018, pp: 1-13.

[12] Bostanabad, R., Bui, A.T., Xie, W., Apley, D.W. and Chen, W., "Stochastic microstructure characterization and reconstruction via supervised learning", *Acta Materialia*, Vol. 103, January 2016, pp: 89-102.

[13] Acar, P., and Sundararaghavan V., "A Markov random field approach for modeling spatio-temporal evolution of microstructures", *Modelling and Simulation in Materials Science and Engineering*, Vol. 24, No. 7, 2016, 075005.

[14] Kumar, A., Nguyen, L., DeGraef, M. and Sundararaghavan, V., "A Markov random field approach for microstructure synthesis", *Modelling and Simulation in Materials Science and Engineering*, Vol. 24, No. 3, 2016, 035015.

[15] Sundararaghavan, V., "Reconstruction of three-dimensional anisotropic microstructures from two-dimensional micrographs imaged on orthogonal planes", *Integrating Materials and Manufacturing Innovation*, Vol. 3, No. 1, 2014, pp: 240-250.

[16] Javaheri, I., and Sundararaghavan, V., "Polycrystalline microstructure reconstruction using Markov random fields and histogram matching", *Computer-Aided Design*, Vol. 120, 2020, 102806.

[17] Javaheri, I., Andani, M. T., and Sundararaghavan, V., "Large-scale synthesis of metal additively-manufactured microstructures using Markov random fields", *Computational Materials Science*, Vol. 206, 2022, 111228.

[18] Xu, H., Dikin, D.A., Burkhart, C. and Chen, W., "Descriptor-based methodology for statistical characterization and 3D reconstruction of microstructural materials", *Computational Materials Science*, Vol. 85, April 2014, pp: 206-216.

[19] Cordero, Z. C., Knight, B. E., and Schuh, C. A., "Six decades of the Hall–Petch effect–a survey of grain-size strengthening studies on pure metals", *International Materials Reviews*, Vol. 61, no. 8, 2016, pp: 495-512.

[20] Wright, S. I., and Nowell, M. M., "EBSD image quality mapping", *Microscopy and microanalysis*, Vol. 12, No. 1, 2006, pp: 72-84.

[21] Wright, S. I., "Fundamentals of automated EBSD", *Electron backscatter diffraction in materials science*, 1st ed., Vol. 2, Springer, Boston, MA, 2000, pp. 51-64.

[22] Schwartz, A.J., Kumar, M., Adams, B.L. and Field, D.P., *Electron backscatter diffraction in materials science*, Vol. 2, Springer, New York, NY, 2009, p. 403.

[23] Adams, B. L., Wright, S. I., and Kunze, K., "Orientation imaging: the emergence of a new microscopy", *Metallurgical Transactions A*, Vol. 24, No. 4, 1993, pp: 819-831.

[24] Dingley, D. J., and Randle, V., "Microtexture determination by electron back-scatter diffraction", *Journal of materials science*, Vol. 27, No. 17, 1992, pp: 4545-4566.

[25] Humphreys, F. J., "Characterisation of fine-scale microstructures by electron backscatter diffraction (EBSD)", *Scripta materialia*, Vol. 51, No. 8, 2004, pp: 771-776.

[26] Bostanabad, R., Zhang, Y., Li, X., Kearney, T., Brinson, L. C., Apley, D. W., Liu, W. K., and Chen, W., "Computational microstructure characterization and reconstruction: Review of the state-of-the-art techniques", *Progress in Materials Science*, Vol. 95, 2018, pp: 1-41.

[27] Senthilnathan, A., and Acar, P., "Shape moment invariants as a new methodology for uncertainty quantification in microstructures", *In AIAA Scitech 2021 Forum*, 2021, p. 1697.

[28] Senthilnathan, A., and Acar, P., "Multi-scale modeling for texture and grain topology of polycrystalline microstructures under uncertainty", *In AIAA SCITECH 2022 Forum*, 2022, p. 2106.

[29] Bernard-Michel, B., Rohani, S., Pons, M.N., Vivier, H. and Hundal, H.S., "Classification of crystal shape using Fourier descriptors and mathematical morphology", *Particle & particle systems characterization*, Vol. 14, No. 4, 1997, pp: 193-200.

[30] Steele, J. H., "Characterizing 3D microstructure using the Minkowski Functionals", *Microscopy and Microanalysis*, Vol. 13, No. S02, 2007, pp: 1658-1659.

[31] Steele, J. H., "The Minkowski Functionals: the global parameters of microstructure", *Microscopy and Microanalysis*, Vol. 10, No. S02, 2004, pp: 712-713.

[32] Inkson, B. J., Mulvihill, M., and Möbus. G., "3D determination of grain shape in a FeAl-based nanocomposite by 3D FIB tomography", *Scripta materialia*, Vol. 45, No. 7, pp: 753-758.

[33] Callahan, P. G., "Quantitative characterization and comparison of precipitate and grain shape in Nickel-base superalloys using moment invariants", Ph.D. Dissertation, Carnegie Mellon University, Pittsburgh, PA, 2012.

[34] Callahan, P. G., Simmons, J. P., and De Graef, M., "A quantitative description of the morphological aspects of materials structures suitable for quantitative comparisons of 3D microstructures", *Modelling and Simulation in Materials Science and Engineering*, Vol. 21, No. 1, 2012, 015003, .

[35] Callahan, P. G., Groeber, M., and De Graef, M., "Towards a quantitative comparison between experimental and synthetic grain structures," *Acta Materialia*, Vol. 111, June 2016, pp: 242-252.

[36] MacSleyne, J. P., "Moment invariants for 2-D and 3-D characterization of the morphology of gamme-prime precipitates in nickel-base superalloys", Ph.D. Dissertation, Carnegie Mellon University, Pittsburgh, PA, 2008.

[37] MacSleyne, J. P., Simmons, J. P., and De Graef, M., "On the use of 2-D moment invariants for the automated classification of particle shapes", *Acta Materialia*, Vol. 56, No. 3, 2008, pp: 427-437.

[38] MacSleyne, J., Uchic, M.D., Simmons, J.P. and De Graef, M., "Three-dimensional analysis of secondary $\gamma^{'}$ precipitates in René-88 DT and UMF-20 superalloys", *Acta Materialia*, Vol. 57, No. 20, 2009, pp: 6251-6267.

[39] De Graef, M., AFRL-AFOSR-VATR-2016-0040.

[40] Nguyen, L., Shi, R., Wang, Y. and De Graef, M., "Quantification of rafting of $\gamma^{'}$ precipitates in Ni-based superalloys", *Acta Materialia*, Vol. 103, January 2016, pp: 322-333.

[41] Nguyen, L., Wang, D., Wang, Y. and De Graef, M., "Quantifying the abnormal strain state in ferroelastic materials: A moment invariant approach", *Acta Materialia*, Vol. 94, August 2015, pp: 172-180.

[42] Senthilnathan, A., Acar, P., and De Graef, M., "Markov random field based microstructure reconstruction using the principal image moments", *Materials Characterization*, Vol. 178, 2021, 111281.

[43] Ising, E., "Beitrag zur theorie des ferromagnetismus", *Zeitschrift für Physik*, Vol. 31, No. 1, 1925, pp: 253-258.